Published in final edited form as:
Nat Genet. 2009 October ; 41(10): 1127–1132. doi:10.1038/ng.438.

Analysis of the Tyrosine Kinome in Melanoma Reveals Recurrent Mutations in ERBB4

Todd D. Prickett[1], **Neena S. Agrawal**[1], **Xiaomu Wei**[1], **Kristin E. Yates**[1], **Jimmy C. Lin**[2], **John Wunderlich**[3], **Julia C. Cronin**[1], **Pedro Cruz**[4], **NISC Comparative Sequencing Program**[4], **Steven A. Rosenberg**[3], and **Yardena Samuels**[1,*]

[1] Cancer Genetics Branch, National Human Genome Research Institute, National Institutes of Health, Bethesda, MD 20892

[2] The Ludwig Center for Cancer Genetics and Therapeutics, the Johns Hopkins Kimmel Cancer Center, Baltimore, MD 21231

[3] Surgery Branch, National Cancer Institute, National Institutes of Health, Bethesda, MD 20892

[4] Genome Technology Branch, National Human Genome Research Institute, National Institutes of Health, Bethesda, MD 20892

Abstract

Tyrosine phosphorylation is important in signaling pathways underlying tumorigenesis. A mutational analysis of the Protein Tyrosine Kinase (PTK) gene family in cutaneous metastatic melanoma identified 30 somatic mutations in the kinase domain of 19 PTKs. The whole of the coding region of these 19 PTKs was further evaluated for somatic mutations in a total of 79 melanoma samples. This analysis revealed novel *ERBB4* mutations in 19% of melanoma patients and that an additional two kinases (*FLT1* and *PTK2B*) are mutated in 10% of melanomas. Seven missense mutations in the most commonly altered PTK (*ERBB4*) were examined and found to increase kinase activity and transformation ability. Melanoma cells expressing mutant ERBB4 had reduced cell growth after shRNA–mediated knockdown of *ERBB4* or treatment with the ERBB inhibitor lapatinib. These studies might lead to personalized therapeutics specifically targeting the kinases that are mutationally altered in individual melanomas.

Malignant melanoma is the most fatal skin cancer [1,2]. To develop personalized treatments for advanced disease, it is important to identify genetic alterations leading to melanoma. Protein tyrosine kinases (PTKs) are frequently mutated in cancer (http://www.sanger.ac.uk/genetics/CGP/Census/), and since they are amenable to pharmacologic inhibition [3,4], further analysis of the PTK gene family may identify new therapeutic strategies. In this study, we used high-throughput gene sequencing to analyze the entire PTK gene family in melanoma, and have identified many novel somatic alterations.

We initially sequenced the coding exons comprising the kinase domains of all 86 members of this gene superfamily in 29 melanomas (Supplementary Table 1). A total of 593 exons were extracted from genomic databases and amplified by polymerase chain reaction (PCR)

[*]To whom correspondence should be addressed: National Human Genome Research Institute, 50 South Drive, MSC 8000, Building 50, Room 5140, Bethesda MD 20892-8000, Phone: 301-451-2628, Fax: 301-480-9864, samuelsy@mail.nih.gov.

Author contributions

T.DP. and Y.S. designed the study; J.R.W. and S.A.R. collected and analyzed the melanoma samples, N.S.A., J.C.C., K.E.Y., J.C.L., NISC., P.C and Y.S. analyzed the genetic data; T.D.P., X.W. and K.E.Y., performed and analyzed the functional data. All authors contributed to the final version of the paper.

from cancer genomic DNA samples using specific primers (Supplementary Table 2) and directly sequenced with dye-terminator chemistry. We determined whether a mutation was somatic (i.e., tumor-specific) by examining the sequence of the gene in genomic DNA from normal tissue of the relevant patient. From the ~12 Mb of sequence information obtained, we identified 19 genes containing a total of 30 somatic mutations within their kinase domains. All coding exons of these 19 genes were then analyzed for mutations in a total of 79 melanoma samples using specific primers (Supplementary Table 3).

We identified 99 non-synonymous, somatic mutations in 19 PTK genes (Table 1 and examples in Supplementary Figure 1 and 3). Only three genes (*EPHA6*, *PDGFRA* and *PTK2*) out of the 19 have previously been reported to be mutated in melanoma (http://www.sanger.ac.uk/genetics/CGP/Census/). The clinical information associated with the melanoma tumors containing somatic PTK mutations is provided in Supplementary Table 4.

The observed somatic mutations could either be “driver” mutations that play a functional role in promoting the neoplastic process or nonfunctional “passenger” changes. In the 19 genes found to be mutated, 99 non-synonymous and 17 synonymous mutations were identified, yielding a N:S (non-synonymous:synonymous) ratio of 5.8:1, significantly higher than the N:S ratio of 2.5:1 predicted for nonselected passenger mutations ($p<1\times10^{-5}$)[5], suggesting that many of these are likely to be “driver” mutations. The number of C>T mutations was significantly greater than other nucleotide substitutions resulting in a high prevalence of C:G>T:A transitions ($p<0.0001$) (Supplementary Figure 2A), confirming previously reported melanoma signatures [6].

To evaluate the effect of some of these mutations on kinase function, we focused on *ERBB4*, the most highly mutated gene in the screen, which harbored 24 somatic mutations (19%). Interestingly, five of the 15 samples with *ERBB4* mutations contained more than one somatic mutation in *ERBB4*, which may act synergistically as previously seen for EGFR [7]. The large number of mutations identified in *ERBB4* strongly suggests that these mutations may be functionally important in melanoma.

Interestingly, 7 out of the 24 non-synonymous somatic mutations discovered in *ERBB4* occurred at Glu (E) residues ($p<0.00005$, binomial test), all of which resulted in changes to Lys (K), causing a charge reversal. The underlying reason for this might be due to the high frequency of C:G>T:A transitions (Supplementary Figure 2B). Clustering of somatic mutations is seen in various functional domains of ERBB4 (Figure 1 and Supplementary Figure 3), with mutations in the kinase domain co-localizing with previously described mutations (found in various cancer types at frequencies ranging from 1.1–4.7% [8,9]) and occurring at highly conserved residues. These genetic data suggest that mutant *ERBB4* is likely to function as an oncogene in melanoma.

To prioritize *ERBB4* missense mutations for further characterization, we assessed the positions of the mutations in its crystal structure[10,11] and found that some of our observed alterations had similar positioning to mutations reported in the *ERBB* family members *EGFR* and *ERBB2* in lung cancer, glioblastoma and gastric cancer [12] (Supplementary Figure 4). Based on this analysis, we chose to evaluate the E317K mutation in the extracellular domain, which is near the EGFR R324L mutation; the E542K, R544W, and E563K mutations which co-localize; the E452K mutation, which was found in two patients; and two mutations in the kinase domain: E836K, which is found near the ERBB2 N857S mutation; and the E872K alteration.

To determine whether the *ERBB4* mutations had enhanced kinase activity, we transiently expressed wild type (WT) ERBB4 or the seven mutants (E317K, E452K, E542K, R544W,

E563K, E836K, E872K) as well as a kinase dead (KD) version of ERBB4 (K751M) in HEK 293T cells and assessed catalytic activity using ERBB4 autophosphorylation (both total and residues Y1162 or Y1284) as a measure of receptor activation. Compared to WT ERBB4, all the missense mutants showed increased phosphorylation of the receptor (Figure 2A). No site-specific phosphorylation was seen in cells exogenously expressing the KD ERBB4. Similar levels of total ERBB4 protein were observed except for KD ERBB4, which was higher (Figure 2A). To determine if the increased tyrosine phosphorylation of the ERBB4 mutants correlates with increased kinase activity, a kinase assay using the same set of ERBB4 mutants was performed. The ERBB4 mutants showed a marked increase in kinase activity compared to WT ERBB4 and expression levels of total ERBB4 protein were comparable (Figure 2B). As in transfected cells, ERBB4 autophosphorylation was markedly elevated in the melanoma lines harboring ERBB4 mutations compared to melanoma lines harboring endogenous WT ERBB4 (Fig 2C–D).

ERBB4 is known to activate several downstream signaling pathways including the ERK and AKT pathways [13]. To evaluate which of these signaling pathways is activated by the ERBB4 mutations, we performed immunoblot analysis of melanoma cell lines harboring endogenous ERBB4 mutations. Phosphorylation of AKT was elevated in cells expressing any of the three evaluated mutant ERBB4s, whereas ERK showed similar activation in cells expressing WT or mutant ERBB4 (Supplementary Figure 5).

To determine whether the ERBB4 variants are transforming, NIH 3T3 cells were transiently transfected with vector, WT ERBB4, one of the seven constitutively active ERBB4 mutants, or oncogenic K-Ras^{G12V}. Ten days after transfection, all ERBB4 mutations transformed NIH 3T3 cells more efficiently than WT ERBB4. Strikingly, the transformation ability of the ERBB4 mutations was similar to oncogenic K-Ras^{G12V} (Figure 3A–B). Similarly, expression of mutant ERBB4 significantly increased anchorage-independent growth as assessed by colony formation in soft agar (Supplementary Figure 6A$p<0.05$, t-test). Similar results were seen for several mutants expressed in the human melanoma cell line SK-Mel-2, which expresses WT ERBB4. Levels of ERBB4 were comparable in all clones (Supplementary Figure 6B).

In order to assess if melanoma cells harboring endogenous ERBB4 mutations are dependent on ERBB4 signaling for proliferation, we used short hairpin RNA (shRNA) to stably knockdown ERBB4 protein levels in melanoma lines harboring either WT (2T and 31T) or mutant ERBB4 (17T, E317K; 63T, E542K/E872K; or 7T, E452K). Specific targeting of ERBB4 by shRNAs was confirmed both in transfected HEK 293 cells and in one of the melanoma cell lines by immunoblotting (Figure 4A–B). Three unique shRNA constructs targeting ERBB4 had minimal effect on the proliferation of cells expressing WT receptor but significantly reduced the growth of melanoma lines containing mutant ERBB4 (Figure 4C–G). Thus, mutant ERBB4 is essential for growth of melanomas harboring these mutations. Evaluation of the effects of ERBB4 knockdown on downstream signaling pathways revealed that down-regulation of ERBB4 in cells harboring mutant versions of the gene reduces levels of endogenous, phosphorylated AKT, but not of phosphorylated ERK. In contrast, inhibition of ERBB4 expression in cells harboring WT versions of the gene showed similar levels of AKT and ERK activation (Supplementary Figure 7).

Because shRNA-mediated cell death could result from specific or nonspecific effects, we examined the ability of an exogenous, non-targetable WT ERBB4 construct (NT ERBB4), engineered to be resistant to knockdown by the introduction of three silent mutations in the region of ERBB4 targeted by shRNA #6, to rescue the effects of knockdown of endogenous ERBB4. Melanoma cells harboring the E317K mutation stably expressing either control or ERBB4 shRNA #6 construct were transduced with the lentiviral NT ERBB4 construct or

empty vector as control. Similar phosphotyrosine content is seen in both WT and NT ERBB4 constructs, demonstrating that the silent mutations in the NT construct do not affect the ability of the receptor to be phosphorylated to wild-type levels (Supplementary Figure 8A). Importantly, pooled clones of NT reconstituted cells were markedly more resistant to growth inhibition induced by ERBB4 knockdown (#6/NT) than shRNA control-infected cells (Vect/Vect).

To evaluate mutant ERBB4 as a potential target for specific inhibition of melanoma cell survival, we targeted the ERBB4 pathway with the FDA-approved pan-ERBB pharmacologic inhibitor, lapatinib (GW2016) [14]. Exposure of melanoma cells to lapatinib resulted in reduced cell proliferation to a greater extent in cells containing endogenous ERBB4 mutations than in cells containing endogenous WT ERBB4 (Figure 5A). An IC_{50} calculation revealed that melanoma cells harboring ERBB4 mutations were 10–250 fold more sensitive to lapatinib than cells with WT receptor (Figure 5B) and treatment with lapatinib inhibited receptor autophosphorylation in a dose-dependent manner (Figure 5C). This increased sensitivity to lapatinib was accompanied by specific inhibition of ERBB4 and AKT activation in cells harboring mutant ERBB4 (Figure 5D–E). Activation of other downstream elements, such as ERK, was also slightly inhibited by lapatinib (Supplementary Figure 9 A–B). Thus, although signaling by mutant ERBB4 demonstrates selective activation of AKT, lapatinib treatment of cells harboring mutant ERRB4 results in uniform inhibition of downstream signaling pathways. Only mutant ERBB4 was inhibited by lapatinib in our melanoma cell lines. No inhibition of its family member ERBB2 was seen (Figure 5D–E) and no phosphorylation of EGFR was observed in any of these cells (data not shown). The observed reduced proliferation occurred in cells harboring BRAF, NRAS, ARAF or CRAF mutations in addition to the ERBB4 mutations (Supplementary Tables 4 and 5).

To elucidate the mechanism of decreased growth of cells expressing mutant ERBB4 following lapatinib treatment, we examined cells for cell cycle perturbations or apoptosis by flow cytometry. Lapatinib markedly increased apoptosis of melanoma cells harboring mutant ERBB4 compared to lines harboring WT ERBB4 (Figure 5F–G). Thus, expression of mutant ERBB4 appears essential for suppression of pro-apoptotic signals in melanoma cells harboring these mutations, which is consistent with the selective activation of AKT in ERBB4 mutant cells (Supplementary Figure 5) and previous results demonstrating an anti-apoptotic role for AKT [15]. These results suggest that lapatinib preferentially inhibits mutant ERBB4 signaling and that cells with ERBB4 mutations are subject to “oncogene addiction” [16]. Moreover, the enhanced AKT signaling in cells with mutant ERBB4 might provide an additional therapeutic target in these tumors.

Previous studies have shown that lapatinib is a much more potent inhibitor of EGFR and ERBB2 (>10X more potent) than ERBB4[11,17–19]. Although lapatinib is clearly leading to a loss of ERBB4 phosphorylation, it is not clear that this is through direct inhibition of ERBB4 kinase activity. It is possible that the inhibitory effects seen by lapatinib are due to ERBB4 transphosphorylation by EGFR and/or ERBB2, and that lapatinib blocks ERBB4 phosphorylation by directly inhibiting EGFR or ERBB2. Alternatively, it is possible that mutant ERBB4 proteins have higher affinity for binding of lapatinib than WT ERBB4. Future work to investigate the mechanism by which lapatinib exerts increased specificity of mutant ERBB4 is warranted.

Here we describe the identification of 99 novel somatic mutations in 19 PTKs in melanoma, few of which had previously been linked to melanoma. The high frequency of mutations identified in *ERBB4*, their co-localization to particular functional domains, as well as the functional studies described above, suggests that these mutations are oncogenic. In contrast

to oncogenes with mutational hotspots, such as *PIK3CA, BRAF and NRAS, ERBB4* mutations occur throughout the gene. Our data and previously reported heterogeneous mutational activation of another oncogene, FLT3, definitively demonstrate that not all mutations in oncogenes must be clustered to be functionally important[20]. Changes that effect enzyme activity can result from single or multiple mutations within a gene that increase activity or abrogate negative regulatory domains. Interestingly, sample 63T harbored two somatic mutations (E542K and E872K) for which the biochemical effects were assessed separately. Both mutations showed increased receptor autophosphorylation and increased kinase activity. These data demonstrate that both mutations exhibit independent, gain-of-function effects, suggesting that the mutations might be synergistic as has been described previously for EGFR [7,21].

Our findings indicate that if future experiments verify that mutational activation of *ERBB4* is essential for tumor growth *in vivo*, targeting of ERBB4 with small-molecule inhibitors should be considered for the large number of patients with these mutations. Broad spectrum ERBB inhibitors, such as lapatinib and canertinib [14,22,23] have already been developed. Our results suggest that further development of such inhibitors is warranted and the clinical utility of this class of compounds be explored in the treatment of melanoma.

Methods

Tumor Tissues

Tissue and melanoma cell lines used in this study were described previously[24].

PCR, sequencing and mutational analysis

PCR and sequencing was done as previously described[24]. The kinase domain mutation screen was analyzed using Consed [25]. Variants were called using Polyphred 6.11[26] and DIP Detector (Hansen N., unpublished), an in del detector for improved sensitivity in finding insertions and deletions.

Sequence traces of the secondary screen were analyzed using the Mutation Surveyor software package (SoftGenetics, State College, PA).

Construction of wild-type and mutant ERBB4 expression vector

Human *ERBB4* (NM_005235) was cloned by PCR as previously described[24] using a clone (#8327667) purchased from Open Biosystems with primers in Supplemental Table 5. The PCR product was cloned into the mammalian expression vector pCDF-MCS2-EF1-Puro™ (Systems Biosciences, Inc., Mountain View, CA) via the XbaI and NotI restriction sites. The E317K, E452K, E542K, R544W, E563K, K751M, E836K, E872K and non-targetable ERBB4 point mutants were made using Phusion PCR for site-directed mutagenesis.

Cell culture and transient expression

Metastatic melanoma tumor lines were maintained as previously described [27]. HEK 293T cells as well as NIH 3T3 were purchased from ATCC (Manassas, VA) and maintained in complete Dulbecco's Modified Eagles Medium (DMEM) supplemented with 10% Fetal Bovine Serum (FBS), 1X non-essential amino acids, 2mM L-glutamine, and 0.75% sodium bicarbonate. HEK 293T cells were transfected with Lipfectamine 2000 reagent (Invitrogen, Carlsbad, CA) at a 6:1 ratio with DNA (μl:μg) using 3–5 μg of plasmid DNA.

Immunoprecipitation and western blotting

Transfected cells were gently washed 3X in PBS and then lysed using 0.5–1.0 ml 1% NP-40 lysis buffer (1% NP-40, 50mM Tris-HCl pH 7.5, 150mM NaCl, Complete Protease Inhibitor tablet, EDTA-free (Roche, Indianapolis, IN), 1μM sodium orthovanadate, 1 mM sodium fluoride, and 0.1% β-mercaptoethanol) per T-75 flask for 20 minutes on ice. Lysed cells were scraped and transferred into a 1.5 mL microcentrifuge tube. Extracts were centrifuged for 10 minutes at 14,000 rpm at 4°C. 500 μl of supernatant was immunoprecipitated overnight using 20 μl of anti-ERBB4 agarose-conjugated beads (Santa Cruz Biotechnology, Inc., Santa Cruz, CA). The immunoprecipitates were washed and subjected to SDS-PAGE and western blotting as previously described [28]. Primary antibodies used in our analysis were anti-ERBB4 (Santa Cruz Biotechnology), anti-P-ERBB4 (Y1162) (Abgent), anti-P-ERBB4 (Y1284) (Cell Signaling, Danvers, MA), anti-PY20 (Zymed-Invitrogen), anti-P-ERK1/2 (T202/Y204), anti-ERK1/2, anti-P-AKT (S473), anti-AKT (Cell Signaling, Danvers, MA), anti-P-STAT5A/B (Y694/Y699) (Upstate Biotech-Millipore), anti-STAT5 (Cell Signaling), and anti-α-tubulin (Calbiochem-EMD Biosciences, Gibbstown, NJ).

Pooled stable expression

To make lentivirus, *ERBB4* constructs were co-transfected into HEK 293T cells seeded at 1.5×10^6 per T75 flask with pVSV-G and pFIV-34N (kind gifts from Todd Waldman, Georgetown University) helper plasmids using Lipofectamine 2000 as described by the manufacturer. Virus-containing media was harvested 48–60hr after transfection, filtered, aliquoted and stored at −80°C.

SK-Mel-2 cells (National Cancer Institute, Division of Cancer Treatment, Developmental Therapeutics Program, Frederick, MD) were grown in RPMI-1640 (Lonza, Walkersville, MD) and supplemented with 10% fetal bovine serum (HyClone, Logan, UT) SK-Mel-2 and NIH 3T3 cells were seeded at 1.5×10^6 cells per T75 flask 24 hr prior to infection. Lentivirus for *ERBB4* (WT, E317K, E452K, E542K, R544W, E563K, K751M, E836K, and E872K point mutants) and empty vector control were used to infect SK-Mel-2 cells or NIH 3T3 cells as previously described[29]. Stable expression of ERBB4 proteins (WT and mutants) was determined by SDS-PAGE analysis followed by immunoblotting with anti-ERBB4 and anti-tubulin to show equivalent expression among pools.

Lentiviral shRNA

Constructs for stable depletion of ERBB4 were obtained from Open Biosystems (Huntsville, AL) and three were confirmed to efficiently knockdown ERBB4 at the protein level. Lentiviral stocks were prepared as previously described[24]. Melanoma cell lines (2T, 7T, 17T, 31T, and 63T) were infected with shRNA lentiviruses for each condition (vector and scrambled controls and three independent *ERBB4*-specific shRNAs). Selection and growth were done as described above. Stably infected pooled clones were tested in functional assays.

To rescue shRNA-mediated knock-down of ERBB4 in melanoma cell lines the non-targetable ERBB4 lentivirus was made as described above and used to infect the melanoma cell line 17T. After infection, cells were given 48 to 72 hours to recover from infection prior to testing in functional assays.

Proliferation and growth inhibition assays

To examine growth potential, melanoma cell lines (2T, 7T, 17T, 31T, and 63T) stably infected with either vector or scrambled controls or ERBB4-specific shRNAs were seeded into 96 well plates at 2,500 cells per well and incubated for 13–17 days. Samples were analyzed every 48 hr by lysing cells in 50 μl 0.2% SDS/well and incubating for 2 hour at

37°C prior to addition of 150 μl/well of SYBR Green I solution (1:750 SYBR Green I (Invitrogen-Molecular Probes) diluted in dH_20).

The effects of tyrosine kinase inhibitors (TKIs) on the proliferation of melanoma cell lines were tested by seeding 96-well plates at 5,000 cells/well in the presence or absence of serum containing media and incubated for 24 hr prior to addition of TKIs. Increasing concentrations of lapatinib (Tykerb-GlaxoSmithKline) were added to each well in four replicates with DMSO as negative control. Plates were analyzed 72 hr post-addition of TKIs using the SYBR Green I proliferation assay described above.

To further test TKIs on melanoma cell lines we seeded 96-well plates at 5,000 cells per well and incubated 24 hr prior to addition of TKIs (e.g. lapatinib) at concentrations from 10 nM to 30 μM. Once inhibitors were added, cells were incubated for 72 hr at 37°C. Cells were then analyzed as previously described[18]. Plates were read at 650nm on a Molecular Devices (Spectra Max) Plate Reader and analyzed using SoftMax v5 and GraphPad Prism v5.

Soft agar assay

SK-Mel-2 pooled ERBB4 clones were plated in duplicate at 1000 cells/well and NIH 3T3 pooled ERBB4 clones were plated in duplicate at 5000 cells/well in top plugs consisting of sterile 0.33% Bacto-Agar (BD, Sparks, MD) and 10% fetal bovine serum (HyClone, Logan, UT) in a 24-well plate. The lower plug contained sterile 0.5% Bacto-Agar and 10% fetal bovine serum. After two weeks, the colonies were photographed and counted.

NIH 3T3 transformation assay

150 ng of each plasmid was transfected by the calcium phosphate precipitation method into NIH 3T3 cells cultured in 12 well plates. 24hr after transfection, 5% of transfected cells were seeded into T-25 flasks and cultured in normal growth medium for 10 days. The cells were stained with Hema3 (Sigma St. Louis, MO) and analyzed for the presence of foci.

Analysis of ERBB4 kinase activity

HEK 293T cells were transiently transfected with ERBB4 (WT, E317K, E452K, E542K, R544W, E563K, E836K, E872K and kinase-dead (K751M)) or empty vector and incubated for 18–24 hr at 37°C in reduced (0.5%) serum containing medium prior to immunoprecipitation. Cells were harvested and ~3 mg of lysate were used in each immunoprecipitation reaction. Immunoprecipitates were performed as described above. Immune complexes were washed three times in lysis buffer followed by two washes in kinase buffer (20 mM HEPES pH 7.4, 50 mM NaCl, 3 mM $MnCl_2$, 20 mM $MgCl_2$, 1 mM sodium orthovanadate, 1 mM sodium fluoride, and 1X complete protease inhibitor tablet). Immune complexes were then resuspended in 50μl kinase buffer and 10μl incubated in the presence of [γ-^{32}P]ATP (3μCi per reaction) for 15 min at 37°C. Kinase reactions were stopped by the addition of 2X SDS sample buffer and phosphorylated samples were resolved on 8% Tris-Glycine gels. Gels were stained and destained prior to autoradiography.

Immunoblot quantitation analysis

Scanned films from western blot analysis of SDS-PAGE were analyzed using ImageJ (NIH software). Individual bands were quantitated and plots were generated to determine the intensities in each band. The data was then exported to Microsoft Excel and analyzed further for phospho:total ratios of protein.

Flow cytometry analysis

Melanoma cells were seeded into T-25 flasks at densities of 3×10^5 cells per flask in normal complete T2 medium and incubated at 37°C for 24 hr prior to addition of lapatinib. Lapatinib or vehicle was added 72 hr at a concentration of 5 μM. Cells were then harvested for FACS analysis by first removing the medium into a new conical tube followed by trypsinizing of attached cells in T-25 flasks. Trypsinized cells and those from the medium were combined and washed in ice-cold PBS. Cells were collected by centrifugation at 1,000 rpm at 4°C. Ice-cold 70% ethanol was added to cell pellets and allowed to fix overnight at 4°C followed by washing in ice-cold PBS. DNase-free RNase (Roche) was to cells resuspended in 0.5–1ml PBS and incubated at 37°C for 30 min before adding 50–100 μl of Propidium Iodide (PI-0.5 mg/ml) (Roche). Cellular DNA content was analyzed on Becton Dickinson FACSCalibur using CellQuest software.

X-ray crystal structure assembly

The X-ray crystal structures of the ERBB4 extracellular and kinase domains were used as templates in the program SWISS-MODEL. Location of EGFR and ERBB2 mutations in the crystal were found by aligning the protein sequences for EGFR, ERBB2, ERBB3, and ERBB4 using ClustalW [30]. Previously known mutations in EGFR and ERBB2 were matched to the sequence of ERBB4 using the ClustalW alignment.

Statistical analysis

To determine whether the ratio of nonsynonymous to synonymous mutations observed was statistically significant, the exact binomial test was used, with an expected ratio of 2.5:1. All the statistical calculations were performed in the R statistical environment (http://www.r-project.org) [5]. Further statistical analyses were performed using Microsoft Excel to generate p-values to determine significance (two-tailed t-test). Inhibition curves (IC_{50}) were analyzed and plotted using GraphPad Prism v5.

Supplementary Material

Refer to Web version on PubMed Central for supplementary material.

Acknowledgments

We thank Drs. Bert Vogelstein, Todd Waldman, Daphne Bell, Paul Meltzer, Larry Brody, Glenn Merlino Silvio Gutkind, and Isabel Cardenas-Navia for their helpful comments on the manuscript. We also thank members of the NISC Comparative Sequencing Program for generating the sequence data analyzed here. We also would like to thank Stacie Anderson and Martha Kirby for assistance with FACS analysis. This work supported by the Intramural Research Programs of the National Human Genome Research Institute and National Cancer Institute, National Institutes of Health

References

1. Jermal A. Cancer Statistics, 2006. CA: A Cancer J Clin 2006;56:106–30.
2. Tsao H, Atkins MB, Sober AJ. Management of cutaneous melanoma. N Engl J Med 2004;351:998–1012. [PubMed: 15342808]
3. Futreal PA, et al. A census of human cancer genes. Nat Rev Cancer 2004;4:177–83. [PubMed: 14993899]
4. Sawyers C. Targeted cancer therapy. Nature 2004;432:294–7. [PubMed: 15549090]
5. Sjoblom T, et al. The consensus coding sequences of human breast and colorectal cancers. Science 2006;314:268–74. [PubMed: 16959974]
6. Greenman C, et al. Patterns of somatic mutation in human cancer genomes. Nature 2007;446:153–8. [PubMed: 17344846]

7. Godin-Heymann N, et al. Oncogenic activity of epidermal growth factor receptor kinase mutant alleles is enhanced by the T790M drug resistance mutation. Cancer Res 2007;67:7319–26. [PubMed: 17671201]
8. Soung YH, et al. Somatic mutations of the ERBB4 kinase domain in human cancers. Int J Cancer 2006;118:1426–9. [PubMed: 16187281]
9. Ding L, et al. Somatic mutations affect key pathways in lung adenocarcinoma. Nature 2008;455:1069–75. [PubMed: 18948947]
10. Bouyain S, Longo PA, Li S, Ferguson KM, Leahy DJ. The extracellular region of ErbB4 adopts a tethered conformation in the absence of ligand. Proc Natl Acad Sci U S A 2005;102:15024–9. [PubMed: 16203964]
11. Qiu C, et al. Mechanism of activation and inhibition of the HER4/ErbB4 kinase. Structure 2008;16:460–7. [PubMed: 18334220]
12. Riese DJ 2nd, Gallo RM, Settleman J. Mutational activation of ErbB family receptor tyrosine kinases: insights into mechanisms of signal transduction and tumorigenesis. Bioessays 2007;29:558–65. [PubMed: 17508401]
13. Frey MR, Edelblum KL, Mullane MT, Liang D, Polk DB. The ErbB4 growth factor receptor is required for colon epithelial cell survival in the presence of TNF. Gastroenterology 2009;136:217–26. [PubMed: 18973758]
14. Heymach JV, Nilsson M, Blumenschein G, Papadimitrakopoulou V, Herbst R. Epidermal growth factor receptor inhibitors in development for the treatment of non-small cell lung cancer. Clin Cancer Res 2006;12:4441s–4445s. [PubMed: 16857825]
15. Grant S, Qiao L, Dent P. Roles of ERBB family receptor tyrosine kinases, and downstream signaling pathways, in the control of cell growth and survival. Front Biosci 2002;7:d376–89. [PubMed: 11815285]
16. Weinstein IB. Cancer. Addiction to oncogenes--the Achilles heal of cancer. Science 2002;297:63–4. [PubMed: 12098689]
17. McHugh LA, et al. Lapatinib, a dual inhibitor of ErbB-1/-2 receptors, enhances effects of combination chemotherapy in bladder cancer cells. Int J Oncol 2009;34:1155–63. [PubMed: 19287975]
18. Rusnak DW, et al. The effects of the novel, reversible epidermal growth factor receptor/ErbB-2 tyrosine kinase inhibitor, GW2016, on the growth of human normal and tumor-derived cell lines in vitro and in vivo. Mol Cancer Ther 2001;1:85–94. [PubMed: 12467226]
19. Xia W, et al. Combining lapatinib (GW572016), a small molecule inhibitor of ErbB1 and ErbB2 tyrosine kinases, with therapeutic anti-ErbB2 antibodies enhances apoptosis of ErbB2-overexpressing breast cancer cells. Oncogene 2005;24:6213–21. [PubMed: 16091755]
20. Shih LY, et al. Heterogeneous patterns of FLT3 Asp(835) mutations in relapsed de novo acute myeloid leukemia: a comparative analysis of 120 paired diagnostic and relapse bone marrow samples. Clin Cancer Res 2004;10:1326–32. [PubMed: 14977832]
21. Pao W, et al. Acquired resistance of lung adenocarcinomas to gefitinib or erlotinib is associated with a second mutation in the EGFR kinase domain. PLoS Med 2005;2:e73. [PubMed: 15737014]
22. Allen LF, Eiseman IA, Fry DW, Lenehan PF. CI-1033, an irreversible pan-erbB receptor inhibitor and its potential application for the treatment of breast cancer. Semin Oncol 2003;30:65–78. [PubMed: 14613028]
23. Sharma SV, Bell DW, Settleman J, Haber DA. Epidermal growth factor receptor mutations in lung cancer. Nat Rev Cancer 2007;7:169–81. [PubMed: 17318210]
24. Palavalli LH, et al. Analysis of the matrix metalloproteinase family reveals that MMP8 is often mutated in melanoma. Nat Genet 2009;41:518–20. [PubMed: 19330028]
25. Gordon D, Abajian C, Green P. Consed: a graphical tool for sequence finishing. Genome Res 1998;8:195–202. [PubMed: 9521923]
26. Bhangale TR, Stephens M, Nickerson DA. Automating resequencing-based detection of insertion-deletion polymorphisms. Nat Genet 2006;38:1457–62. [PubMed: 17115056]
27. Chappell DB, Zaks TZ, Rosenberg SA, Restifo NP. Human melanoma cells do not express Fas (Apo-1/CD95) ligand. Cancer Res 1999;59:59–62. [PubMed: 9892185]

28. Samuels Y, et al. High frequency of mutations of the PIK3CA gene in human cancers. Science 2004;304:554. [PubMed: 15016963]

29. Solomon DA, et al. Mutational inactivation of PTPRD in glioblastoma multiforme and malignant melanoma. Cancer Res 2008;68:10300–6. [PubMed: 19074898]

30. Guex N, Peitsch MC. SWISS-MODEL and the Swiss-PdbViewer: an environment for comparative protein modeling. Electrophoresis 1997;18:2714–23. [PubMed: 9504803]

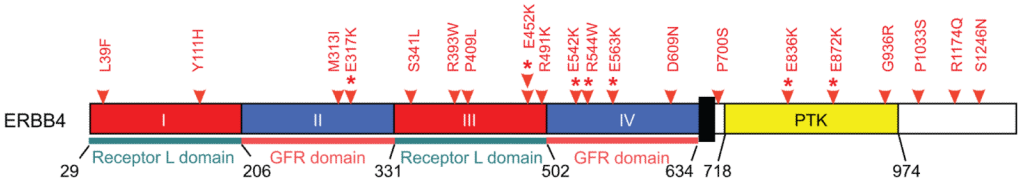

Figure 1. Distribution of mutations in ERBB4

Red arrows indicate the location of ERBB4 somatic mutations found in this screen. Red stars indicate ERBB4 mutants used in subsequent analysis. Boxes represent functional domains (I, Extracellular Domain Subregion I; II, Extracellular Domain Subregion II; III, Extracellular Domain Subregion III; IV, Extracellular Domain Subregion IV; Kinase, Tyrosine Kinase Domain).

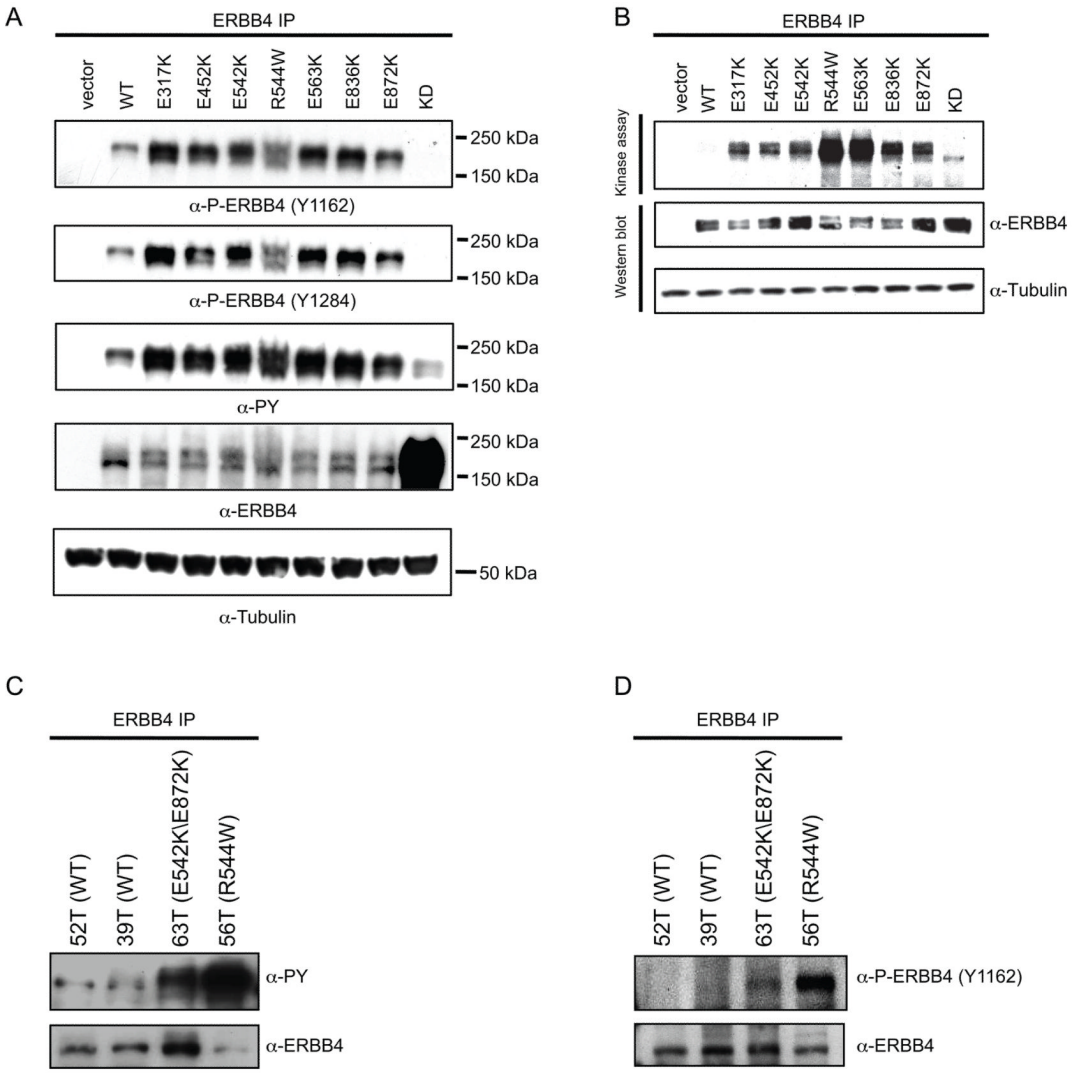

Figure 2. ERBB4 mutants exhibit increased basal activation

A. ERBB4 mutants have increased tyrosine phosphorylation. HEK 293T cells were transiently transfected with the indicated constructs. 24 hrs after transfection, cells were serum starved, lysed and immunoprecipitated with α-ERBB4. After immunoprecipitation of ERBB4, immunoblots were performed using specific antibodies, as indicated. Lysates were immunoblotted with an α-tubulin antibody. B. ERBB4 mutants exhibit increased *in vitro* kinase activity. HEK 293T cells were transiently transfected as in A. Equivalent amounts of protein from cell lysates were immunoprecipitated and used in a kinase assay to measure receptor autophosphorylation. The same samples that were used in the kinase assay were immunoblotted with ERBB4 antibody and lysates were blotted with α-tubulin. KD: kinase dead. C. Increased basal activation of endogenous mutant ERBB4. Melanoma lines that harbor either WT or mutant ERBB4 were serum starved and then lysed, immunoprecipitated for ERBB4, then immunoblotted withα-PY20 or α-ERBB4. D. Mutant ERBB4 has increased basal activity. Melanoma lines harboring either WT or mutant ERBB4 were serum deprived, lysed, immunoprecipitated for ERBB4, and analyzed by immunoblotting with α-P-ERBB4 (P-Y1162) or α-ERBB4.

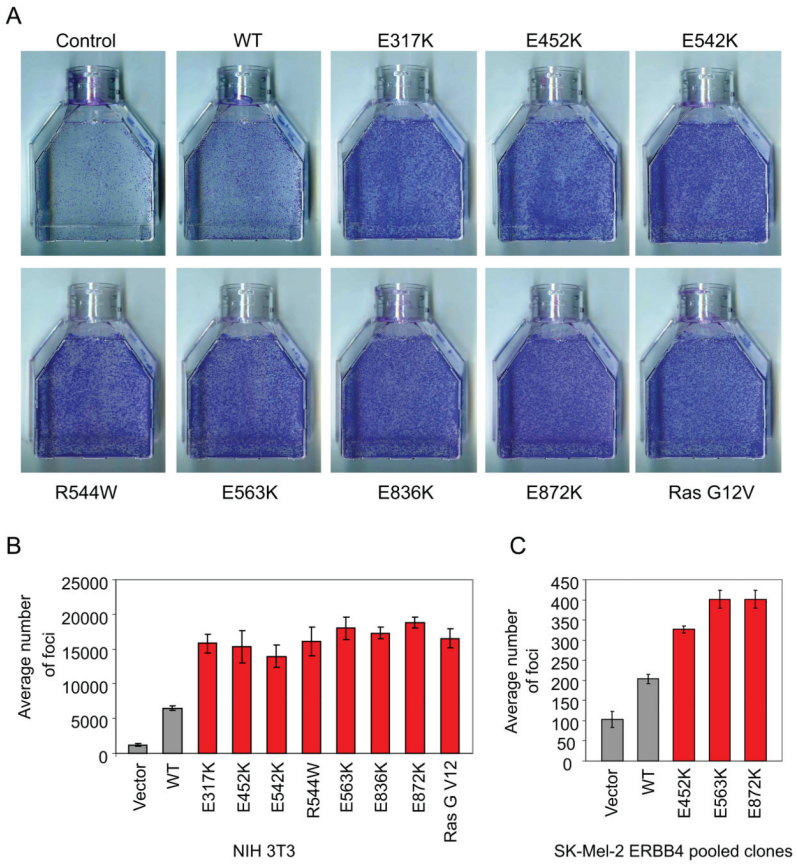

Figure 3. Mutant ERBB4 induces cell transformation and anchorage-independent growth in NIH 3T3 and SK-Mel-2 cells

A. NIH 3T3 cells were transfected with the indicated constructs. The photographs show foci stained with Hema3 after 10 days. Ras ^{G12V} was included as a positive control for cell transformation. B. The graph indicates the average number of foci visualized in A. C. Transformation ability of melanoma SK-Mel-2 cells stably expressing either vector, WT ERBB4 or various ERBB4 missense mutants was assessed by foci formation in tissue culture flasks. The graph indicates the number of foci formed after 14 days.

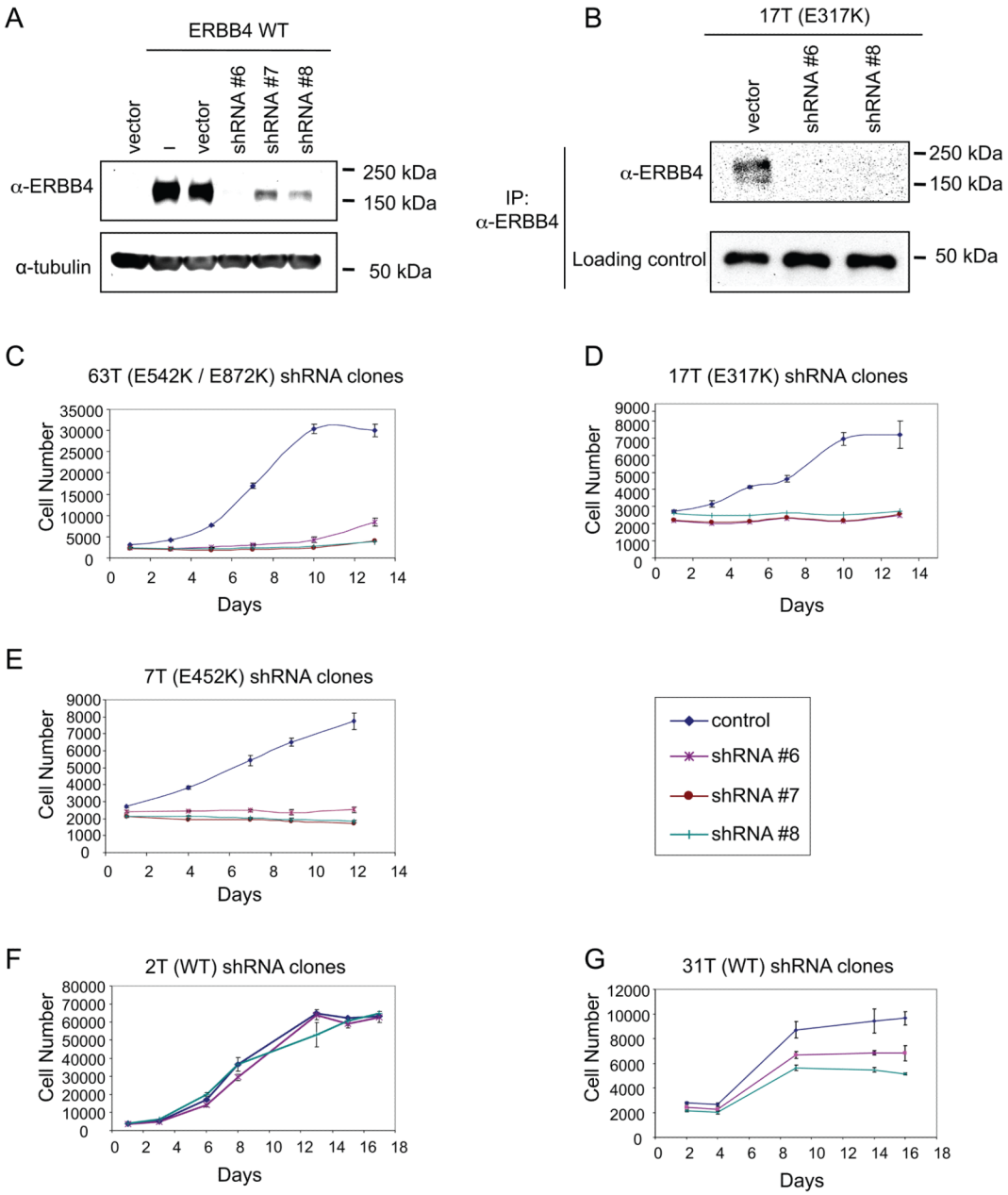

Figure 4. Expression of mutant ERBB4 provides an essential cell survival signal in melanoma

A. HEK 293 cells were transiently co-transfected with either vector or WT ERBB4 together with either control vector or shRNAs that target ERBB4. Cell lysates were analyzed by immunoblotting using α-ERBB4. For normalization, lysates were analyzed in parallel by α-tubulin immunoblotting. B. Cells transduced with shRNA targeting ERBB4 were lysed and immunopreciptitated using α-ERBB4 beads. Immunoprecipitates were blotted with specific antibodies, as indicated. C–G. shRNA-mediated ERBB4 knockdown in melanoma lines containing ERBB4 mutations results in reduced cell growth. Cells were seeded in 96-well plates and incubated for 13–17 days. Plates were analyzed every other day for cell proliferation where the average cell number at each time point was measured by determining DNA content using SYBR Green I. Melanoma cells harboring ERBB4 mutations stably transduced with shRNA constructs targeting ERBB4, but not those stably transduced with

the control vector only, showed decreased growth relative to control. This did not occur in melanoma cells harboring WT ERBB4.

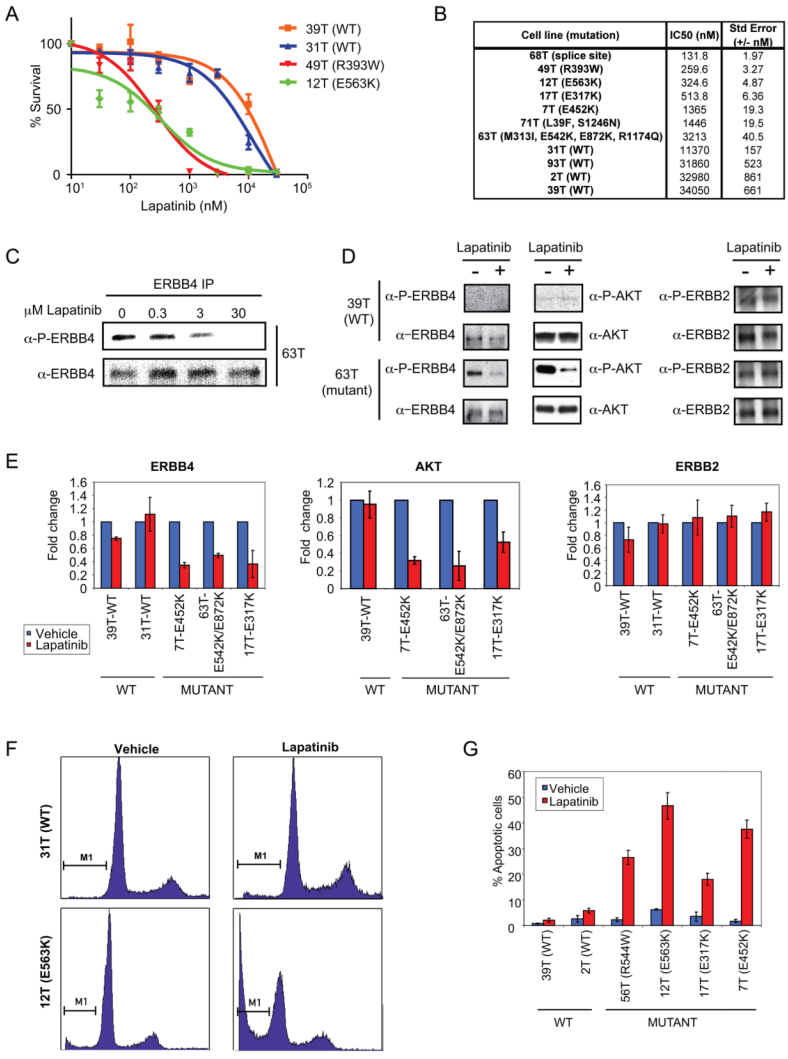

Cell line (mutation)	IC50 (nM)	Std Error (+/- nM)
68T (splice site)	131.8	1.97
49T (R393W)	259.6	3.27
12T (E563K)	324.6	4.87
17T (E317K)	513.8	6.36
7T (E452K)	1365	19.3
71T (L39F, S1246N)	1446	19.5
63T (M313I, E542K, E872K, R1174Q)	3213	40.5
31T (WT)	11370	157
93T (WT)	31860	523
2T (WT)	32980	861
39T (WT)	34050	661

Figure 5. Melanoma lines expressing ERBB4 mutants exhibit increased sensitivity to ERBB inhibition by lapatinib

A. Representative dose response curves showing lapatinib efficacy against ERBB4 mutant lines compared to WT ERBB4 lines. Cells were treated for 72 hours in the presence of increasing concentrations (0.01–30 μM) of lapatinib, and relative cell number was estimated by methylene blue protein staining and plotted as percent survival when compared to vehicle-treated control versus Log (lapatinib) nM (where 1 is 10 nM lapatinib). Fitted lines were generated using 4-parameter nonlinear regression via GraphPad Prism. B. ERBB4 mutant lines have increased sensitivity to lapatinib compared to WT ERBB4 lines. The IC_{50} values for inhibition of cell growth by 72 hr treatment with lapatinib of a larger panel of lines harboring WT and mutant ERBB4 were analyzed using GraphPad Prism v.5 (n=3). C. Immunoprecipitation and western blot analysis of ERBB4 autophosphorylation in cells treated with lapatinib. Cells were treated for 1 hr with lapatinib or vehicle alone as control. Lysates were immunoprecipitated with α-ERBB4 followed by western blot analysis with α-ERBB4 and α-P-ERBB4 (Y1162). D. Melanoma lines expressing mutant ERBB4 exhibit increased lapatinib sensitivity with respect to ERBB4 as well as AKT phosphorylation. The activity of ERBB4, AKT as well as ERBB2 was determined by immunoblotting with phospho-specific antibodies. Cells were treated for 1 hr with 5 μM lapatinib or vehicle alone. Lysates were immunoprecipitated using α-ERBB2 or α-ERBB4. Lysates and

immunoprecipitates were analyzed by western blotting using the indicated antibodies. Shown are representative blots. E. Quantitative assessment of data from 2 lines harboring WT ERBB4 and 3 lines harboring mutant ERBB4 that were performed similarly to D. D. The ratio of band intensities of (P-Y1162)-ERBB4/ERBB4, (P)-S473-AKT/AKT and (P-Y1248)-ERBB2/ERBB2 for each cell line are shown. F. Mutant ERBB4 cells have increased sub-G1 population in the presence of lapatinib compared to WT ERBB4 cells. FACS analysis of 31T (WT) and 12T (E563K) showing cell cycle distribution (PI staining, x-axis) vs cell counts (y-axis). Shown are representative plots. G. Quantitation of FACS-sorted lapatinib-treated cells. The percent apoptotic cells were determined based on the sub G1 population for vehicle treated cells or lapatinib treated cells.

Nat Genet. Author manuscript; available in PMC 2010 July 6.

Table 1

Somatic mutations Identified in PTK-s

Gene	CCDS accession*	Ref Seq accession*	No. of mutations#	% of cases affected#	Exon	Nucleotide†	Amino Acid†	Functional Domain	Tumor	NRAS/BRAF mutation**
DDR1	CCDS4690.1	NM_001954.3	2	2.5	8	C1115T	S372F	None	6T	BRAF
					11	G1709A	R570Q	Protein Tyrosine Kinase	43T	BRAF
FER	CCDS4098.1	NM_005246.1	2	2.5	11	T1594C	Y532H	SH2 Motif	58T	BRAF
					13	G1739A	G580D	Protein Tyrosine Kinase	30T	BRAF
FLT1	CCDS9330.1	NM_002019.3	8	10.1	7	G842A	R281Q	IG	37T	BRAF
					7	C860T	S287F	IG	7T	NRAS
					12	−9 Intronic C>A	Splice Site	N/A	20T	BRAF
					13	G1767A	W589X	IGc2	13T	None
					17	C2440T	P814S	None	39T	None
					21	G2827A	E943K	Protein Tyrosine Kinase	44T	NRAS
					24	G3241A	D1081N	Protein Tyrosine Kinase	78T	BRAF
					28	G3667A	E1223K/LOH	None	85T	BRAF
EPHA6		NM_001080448.2	5	6.3	1	C1202G	T307S	None	30T	BRAF
					4	G1763T	R494M	Protein Tyrosine Kinase	36T	BRAF
					4	G1891A	E537K	Protein Tyrosine Kinase	32T	BRAF
					8	A2246T	K655I	Protein Tyrosine Kinase	29T	BRAF
					8	G2320A	E680K	None	21T	BRAF
EPHA10	CCDS41305.1	NM_001099439.1	7	6.3	3	G235A	V79M	Ephrin Receptor	52T	BRAF
					3	T236C	V79A	Ephrin Receptor	52T	BRAF
					3	G370A	E124K	Ephrin Receptor	55T	None
					3	G649A	G217S	None	71T	BRAF
					3	G650A	G217D	None	71T	BRAF
					13	G2369A	G790E	Protein Tyrosine Kinase	63T	NRAS
					14	G2528C	G843A	Protein Tyrosine Kinase	37T	BRAF
EPHB1		NM_004441	4	5.1	3	C235T	R79W	Ephrin Receptor	39T	None
					12	G2311A	D771N	Protein Tyrosine Kinase	60T	NRAS
					13	G2432A	G811E	Protein Tyrosine Kinase	44T	NRAS

Gene	CCDS accession*	Ref Seq accession*	No. of mutations#	% of cases affected#	Exon	Nucleotide†	Amino Acid†	Functional Domain	Tumor	NRAS/BRAF mutation**
					15	G2757A	W919X	Sterile Alpha Motif	63T	NRAS
EPHB2	CCDS229.2	NM_017449.1	7	8.9	3	G325A	E109K	Ephrin Receptor	4T	BRAF
					3	C614T	A205V	None	72T	None
					4	G952A	D318N	Fibronectin Type 3 Domain	71T	BRAF
					7	C1535T	T512I	Fibronectin Type 3 Domain	83T	Both
					10	G1846A	E615K	Protein Tyrosine Kinase	29T	BRAF
					10	G1846A	E615K	Protein Tyrosine Kinase	68T	BRAF
					14	C2663T	P887L	None	77T	None
EPHB6	CCDS5873.1	NM_004445.1	7	8.9	3	C392T	S131F	Ephrin Receptor	60T	NRAS
					3	C455T	S152F	Ephrin Receptor	55T	None
					5	G1210A	G404S	Fibronectin Type 3 Domain	50T	BRAF
					11	G2036A	R679Q	Protein Tyrosine Kinase	5T	BRAF
					11	C2063G	A688G	Protein Tyrosine Kinase	54T	BRAF
					11	C2110T	R704W	Protein Tyrosine Kinase	26T	BRAF
					13	−5 Intronic C>T	Splice Site	N/A	18T	None
ERBB4	CCDS2394.1	NM_005235.2	24	19.0	2	C113T	L39F	Receptor L Domain	71T	BRAF
					3	T331C	Y111H	Receptor L Domain	13T	None
					8	G939A	M313I	Growth Factor Receptor	63T	NRAS
					8	G949A	E317K	Growth Factor Receptor	17T	NRAS
					9	C1022T	S341L	Receptor L Domain	96T	None
					10	C1177T	R393W	Receptor L Domain	49T	BRAF
					11	C1226T	P409L	Receptor L Domain	76T	None
					12	G1354A	E452K	Receptor L Domain	7T	NRAS
					12	G1354A	E452K/LOH	Receptor L Domain	55T	None
					12	G1472A	R491K/LOH	Growth Factor Receptor	34T	BRAF
					14	G1624A	E542K	Growth Factor Receptor	63T	NRAS
					14	C1630T	R544W	Growth Factor Receptor	56T	BRAF
					14	G1687A	E563K	Growth Factor Receptor	12T	NRAS
					15	−10 Intronic C>T	Splice Site/LOH	N/A	68T	BRAF
					15	G1825A	D609N	Growth Factor Receptor	76T	None

Gene	CCDS accession*	Ref Seq accession*	No. of mutations#	% of cases affected#	Exon	Nucleotide†	Amino Acid†	Functional Domain	Tumor	NRAS/BRAF mutation**
					18	C2098T	P700S	None	24T	NRAS
					21	G2506A	E836K	Protein Tyrosine Kinase	86T	BRAF
					21	G2614A	E872K	Protein Tyrosine Kinase/Activation Loop	63T	NRAS
					23	G2806A	G936R	Protein Tyrosine Kinase	24T	NRAS
					24	−4 Intronic C>T	Splice Site	N/A	13T	None
					25	C3097T	P1033S	None	76T	None
					26	−1 Intronic G>A	Splice Site	N/A	76T	None
					28	G3521A	R1174Q	None	63T	NRAS
					28	G3737A	S1246N	His-Me Finger Endonucleases	71T	BRAF
MATK	CCDS12113.1	NM_002378.2	1	1.3	12	G1248A	W416X	Protein Tyrosine Kinase	13T	None
MET	CCDS43636.1	NM_000245	3	3.8	5	G1829A	C610Y/LOH	IPT	1T	BRAF
					14	A3176G	N1059S	None	13T	None
					16	G3509A	R1170Q	Protein Tyrosine Kinase	29T	BRAF
NTRK1	CCDS1161.1	NM_002529.2	2	2.5	8	G1137A	M349I	None	18T	None
					14	C1747G	R547G	Protein Tyrosine Kinase	13T	None
PDGFRA	CCDS3495.1	NM_006206.2	5	5.1	3	G571A	A191T	IG	64T	BRAF
					9	G1375A	E459K/LOH	None	32T	BRAF
					18	C2669T	S890F	Protein Tyrosine Kinase	41T	BRAF
					20	C2810T	P937L/LOH	Protein Tyrosine Kinase	32T	BRAF
					21	G3070A	D1024N	None	63T	NRAS
PTK2	CCDS6381.1	NM_153831.2	1	1.3	15	C1481T	A494V	Protein Tyrosine Kinase	13T	None
PTK2B	CCDS6057.1	NM_173176.1	8	10.1	5	−4 Intronic C>T	Splice Site	N/A	79T	BRAF
					8	G818A	W273X	FERM	76T	None
					13	G1241A	G414E	None	95T	NRAS
					14	C1285T	R429C	Protein Tyrosine Kinase	17T	NRAS
					16	G1480A	E494K	Protein Tyrosine Kinase	26T	BRAF
					24	G2374A	E792K	None	36T	BRAF
					29	G2753A	R918Q	Focal AT	85T	BRAF
					29	G2812A	E938K	Focal AT	83T	Both

Gene	CCDS accession*	Ref Seq accession*	No. of mutations#	% of cases affected#	Exon	Nucleotide†	Amino Acid†	Functional Domain	Tumor	NRAS/BRAF mutation**
PTK6	CCDS13524.1	NM_005975.2	2	2.5	4	G629A	W210X	Protein Tyrosine Kinase	12T	NRAS
					5	−7 Intronic C>T	Splice Site	N/A	51T	BRAF
PTK7	CCDS4884.1	NM_002821.3	1	1.3	7	C1054T	P352S	IGc2	84T	BRAF
ROR2	CCDS6691.1	NM_004560.2	4	5.1	5	T574C	Y192H	Frizzled Cysteine-Rich Domain	71T	BRAF
					7	T1172C	V391A	Kringle	72T	None
					9	C1670T	S557L	Protein Tyrosine Kinase	5T	BRAF
					9	G2377T	A793S	None	81T	BRAF
TIE1	CCDS482.1	NM_005424.2	6	7.6	2	G139A	E47K	None	13T	None
					2	C161T	S54L	None	16T	BRAF
					2	C266T	T89M	None	52T	BRAF
					2	G292A	D98N	None	43T	BRAF
					11	G1598A	G533E	Fibronectin Type 3 Domain	39T	None
					22	C3281T	P1094L/LOH	Protein Tyrosine Kinase	12T	NRAS

*Accession numbers for mutated PTK-s in Santa Cruz and GenBank.

#Number of non-synonymous and splice site mutations observed and percent of tumors affected for each of the 19 genes in the panel of 79 melanoma cancers.

†Nucleotide and amino acid change resulting from mutation.

"X" refers to stop codon. "LOH" refers to cases wherein the wild-type allele was lost and only the mutant allele remained. "Splice site" refers to a case wherein the alteration affected ten bases spanning the exon.

**Mutations previously observed in NRAS, or BRAF.

"None" refers to no mutation observed. SH2 Motif, Src homology 2 domain; IG, Immunoglobin; IGc2, Immunoglobin C-2 Type; IPT, IG-like, plexins, transcription factors; Focal AT, Focal Adhesion Targeting Region; FERM, Protein 4.1, Ezrin, Radixin, Moesin Domain. Domains were found using Ensembl and InterPro.